

# ASYMPTOTIC GENERALIZED EIGENVALUE DISTRIBUTION OF BLOCK TOEPLITZ MATRICES AND APPLICATION TO SPACE-TIME BEAMFORMING

Marc Oudin, Jean-Pierre Delmas

GET/INT, Département CITI, UMR-CNRS 5157  
9 rue Charles Fourier, 91011 Evry Cedex, France  
phone: +(33).1.60.76.45.44, +(33).1.60.76.46.32, fax: +(33).1.60.76.44.33  
marc.oudin@int-edu.eu, jean-pierre.delmas@int-edu.eu

## ABSTRACT

*In many detection applications, the main performance criterion is the Signal to Interference plus Noise Ratio (SINR). After linear filtering, the optimal SINR corresponds to the maximum value of a Rayleigh quotient, which can be interpreted as the largest generalized eigenvalue of two covariance matrices. In this paper, we extend the Szegő's theorem for the generalized eigenvalues of Hermitian block Toeplitz matrices derived under the assumption of absolutely summable sequences. Then, we apply this result to wideband space-time beamforming performance analysis where the optimal SINR can be interpreted as the largest generalized eigenvalue of a block Toeplitz matrices' pair. We show that the optimal space-time SINR converges to an upper bound that can be interpreted as an optimal zero-bandwidth spatial SINR and interpret this result for several jamming scenarios.*

## 1. INTRODUCTION

In many detection applications, such as radar and sonar, the main performance criterion is the Signal to Interference plus Noise Ratio (SINR). If a linear filter is applied to data, the SINR corresponds to a Rayleigh quotient, associated with the covariance matrices of the signal and interference plus noise components. In many applications, those matrices may be structured. For instance, in the case of temporal filtering, if the data are modelled by stationary processes, they will be Toeplitz structured. Another example is the case of space-time filtering where the two matrices are block Toeplitz structured.

In this paper, we study the problem of the influence of the filter order on the optimal SINR. More specifically, we consider the case of block Toeplitz matrices. Because the optimal SINR corresponds to the maximum value of a Rayleigh quotient, it can be interpreted as the largest generalized eigenvalue of both matrices. Therefore, the problem of the influence of the filter order on the SINR is closely related to the generalized eigenvalue problem which has, to the best of our knowledge, received little attention in the signal processing literature. In numerical analysis, a similar problem deals with the analysis of the behavior of the eigenvalues of a preconditioned matrix. For this problem, results about the asymptotic behavior of the eigenvalues of block Toeplitz matrices have been derived [2, 3]. They extend the celebrated result given by Szegő [4], which asserts that the eigenvalues of a sequence of Hermitian Toeplitz matrices asymptotically behave like the samples of the Fourier transform of its entries. However, the analyses have been performed by use of sophisticated mathematics under the general hypothesis that the block matrices are generated by square summable elements.

Here, we propose to extend the Szegő's theorem to the generalized eigenvalues of block Toeplitz matrices, under the hypothesis of absolutely summable elements. This extension relies on the asymptotic equivalence of matrix sequences established by Gray in [5]. Then, we apply this theorem to the performance analysis of the maximal SINR space-time (or tapped delay line) wideband beamformer (e.g., see [6, Chap. 6.13]). We derive the expression of the asymptotic optimal space-time SINR w.r.t. the number of taps and show that it can outperform the optimal associated zero-bandwidth

spatial SINR. This result is illustrated by numerical simulations, as well as the convergence to the asymptotic SINR with a finite number of taps. We may note that many authors have studied the performance of wideband beamformers, using time domain or frequency domain implementations. However, to the best of our knowledge, they have considered different weight optimization criteria, such as the Minimum Mean Square Error (MMSE) or Minimum Variance with Distortionless Response (MVDR) (e.g., see [7, 8]). Moreover, most analyses have been done through numerical simulations (e.g., see [7, 9]) and few analytical results exist. Furthermore, they were performed for particular cases of arrays with a limited number of sensors (e.g., see [8]). Contrary to the previous studies, our asymptotic approach allows us to consider arbitrary arrays with an arbitrary number of sensors.

## 2. GENERALIZED EIGENVALUE PROBLEM

In this section, we review the generalized eigenvalue problem and provide some insights into two cases appearing frequently in signal processing applications.

### 2.1 Stationary points of Rayleigh quotient

Given two  $n \times n$  Hermitian matrices  $\mathbf{A}$ ,  $\mathbf{B}$  and an  $(n \times 1)$  vector  $\mathbf{w}$ , with  $\mathbf{B}$  positive definite, the Rayleigh quotient is defined as the ratio

$$r(\mathbf{w}) = \frac{\mathbf{w}^H \mathbf{A} \mathbf{w}}{\mathbf{w}^H \mathbf{B} \mathbf{w}}. \quad (1)$$

This ratio is closely related to the generalized eigenvalue problem. Its stationary points can be interpreted as the generalized eigenvectors of the matrices  $\mathbf{A}$  and  $\mathbf{B}$ . Indeed, by taking the complex gradient of (1) w.r.t.  $\mathbf{w}$  and setting the result to zero, we obtain

$$\mathbf{A} \mathbf{w} = r(\mathbf{w}) \mathbf{B} \mathbf{w}$$

which is the expression of a generalized eigenproblem. Therefore, the stationary points  $\mathbf{w}$  and stationary values  $r(\mathbf{w})$  of the Rayleigh quotient are, respectively, the generalized eigenvectors and eigenvalues  $\lambda(\mathbf{A}, \mathbf{B})$  of the corresponding generalized eigenproblem. Moreover, since  $\mathbf{B}$  is positive definite, the previous expression is equivalent to

$$\mathbf{B}^{-1} \mathbf{A} \mathbf{w} = r(\mathbf{w}) \mathbf{w}$$

and the generalized eigenvectors and eigenvalues of  $\mathbf{A}$  and  $\mathbf{B}$  respectively, correspond to the eigenvectors and eigenvalues of  $\mathbf{B}^{-1} \mathbf{A}$ , i.e.,  $\lambda(\mathbf{A}, \mathbf{B}) = \lambda(\mathbf{B}^{-1} \mathbf{A})$ .

### 2.2 Toeplitz and block Toeplitz case

Applied to statistics, the matrices  $\mathbf{A}$  and  $\mathbf{B}$  can be interpreted as the covariance matrices of stochastic processes and therefore Hermitian positive semidefinite. Very frequently, stochastic processes are the sum of two zero-mean stochastic processes: the process of interest and the noise process of covariance matrices  $\mathbf{A}$  and  $\mathbf{B}$  respectively. In this case, the Rayleigh quotient (1) can be interpreted as a SINR after application of a linear filter to the stochastic processes. In this situation  $\mathbf{B}$  is almost always positive definite and a question of

interest is the maximization of this quotient (1) for different orders of the linear filter.

Two significant particular cases can be developed, depending on the properties of the processes and the sampling. First, in the case of a temporal periodic sampling of stationary processes, the covariance matrices are Toeplitz. Next, in the case of space-time sampling, the matrices are block Toeplitz if the sampling order is spatial then temporal or Toeplitz block otherwise (i.e. temporal then spatial). In the following, we restrict ourselves to the generalized eigenvalue analysis of the latter kind of matrices.

### 3. ASYMPTOTIC GENERALIZED EIGENVALUE DISTRIBUTION OF BLOCK TOEPLITZ MATRICES

The aim of this Section is to extend Szegő's theorem [4] to the case of the generalized eigenvalues of block Toeplitz matrices under the hypothesis that the elements generating the matrices are absolutely summable. For this purpose, we start by explaining notations and recall previous results useful for the proof of this theorem (Theorem 1).

#### 3.1 Notations and previous results

Depending on the order the data are written, the matrices can be block Toeplitz or Toeplitz block structured for which it is straightforward to prove that the associated pairs share the same generalized eigenvalues. However, the formulation of Toeplitz block is preferred as it allows one to handle Toeplitz block for which Lemma 1 will apply. Thus, let  $\mathbf{A}_{n,m}$  denote a Hermitian Toeplitz block matrix and  $\mathbf{B}_{n,m}$  a Hermitian, positive definite Toeplitz block matrix with

$$\mathbf{A}_{n,m} = \begin{bmatrix} \mathbf{A}_n^{1,1} & \mathbf{A}_n^{1,2} & \dots & \mathbf{A}_n^{1,m} \\ \mathbf{A}_n^{2,1} & \mathbf{A}_n^{2,2} & \dots & \mathbf{A}_n^{2,m} \\ \vdots & \vdots & \ddots & \vdots \\ \mathbf{A}_n^{m,1} & \mathbf{A}_n^{m,2} & \dots & \mathbf{A}_n^{m,m} \end{bmatrix}$$

where  $(\mathbf{A}_n^{u,v})_{u=1..m,v=1..m}$  denote  $n \times n$  Toeplitz matrices given by

$$\mathbf{A}_n^{u,v} = \begin{bmatrix} a_0^{u,v} & a_{-1}^{u,v} & \dots & a_{-(n-1)}^{u,v} \\ a_1^{u,v} & \ddots & \ddots & a_{-(n-2)}^{u,v} \\ \vdots & \ddots & \ddots & \vdots \\ a_{n-1}^{u,v} & a_{n-2}^{u,v} & \dots & a_0^{u,v} \end{bmatrix} \quad (2)$$

where  $\{a_k^{u,v}\}_{k=-\infty,-1,0,1,\dots}$  are absolutely summable infinite complex sequences, which guarantees the existence of the associated  $2\pi$  periodic Fourier transform  $a^{u,v}(\omega) = \sum_k a_k^{u,v} e^{-ik\omega}$ . Finally, we introduce the spectral matrix of elements  $[\mathbf{A}(\omega)]_{u,v} = a^{u,v}(\omega)$ ,  $u, v = 1..m$ . These notations extend to the Toeplitz block matrices  $\mathbf{B}_{n,m}$ .

To study the asymptotic behavior of sequences of matrices, two norms have been introduced in [5]. They are the spectral norm  $\|\cdot\|$  and the normalized Frobenius norm  $|\cdot|$

$$|\mathbf{A}_n|^2 \stackrel{\text{def}}{=} \frac{1}{n} \sum_{i=1}^n \sum_{j=1}^n |a_{i,j}|^2.$$

Both norms are used for the definition of asymptotic equivalence given in [5]:

**Definition:** Two matrix sequences  $\{\mathbf{A}_n\}$  and  $\{\mathbf{B}_n\}$ ,  $n = 1, 2, \dots$  are said to be asymptotically equivalent,  $\mathbf{A}_n \sim \mathbf{B}_n$  if

1.  $\exists M < \infty$  such that  $\forall n$ ,  $\|\mathbf{A}_n\| \leq M$  and  $\|\mathbf{B}_n\| \leq M$
2.  $\lim_{n \rightarrow \infty} |\mathbf{A}_n - \mathbf{B}_n| = 0$ .

We now recall a lemma about block Toeplitz matrices [10] that will be useful in the following:

**Lemma 1** For all absolutely summable sequences  $\{a_k^{u,v}\}_{k=-\infty,-1,0,1,\dots}$  there exists a sequence of matrices  $\{\mathbf{C}_n(a)\}$  asymptotically equivalent to  $\{\mathbf{A}_{n,m}\}$  and given by

$$\mathbf{C}_n(a) = \mathbf{U}_{n,m}^H \Delta_n(a) \mathbf{U}_{n,m}$$

where  $\mathbf{U}_{n,m} = \mathbf{I}_m \otimes \mathbf{U}_n$  is an  $nm \times nm$  unitary matrix independent of  $\mathbf{A}_{n,m}$  with  $\mathbf{U}_n$  the unitary discrete Fourier transform (DFT) matrix and where  $\Delta_n(a)$  is the following matrix:

$$\Delta_n(a) \stackrel{\text{def}}{=} \begin{bmatrix} \mathbf{D}_n(a^{1,1}) & \mathbf{D}_n(a^{1,2}) & \dots & \mathbf{D}_n(a^{1,m}) \\ \mathbf{D}_n(a^{2,1}) & \mathbf{D}_n(a^{2,2}) & \dots & \mathbf{D}_n(a^{2,m}) \\ \vdots & \vdots & \ddots & \vdots \\ \mathbf{D}_n(a^{m,1}) & \mathbf{D}_n(a^{m,2}) & \dots & \mathbf{D}_n(a^{m,m}) \end{bmatrix}$$

where  $\mathbf{D}_n(a^{u,v})$  are diagonal matrices with their  $k^{\text{th}}$  entry given by  $(\mathbf{D}_n(a^{u,v}))_{k,k} = a^{u,v} \left( \frac{2\pi(k-1)}{n} \right)$ .

#### 3.2 Asymptotic generalized eigenvalue distribution of block Toeplitz matrices

After having recalled useful previous results, we now give in Theorem 1 the extension of Szegő's theorem to the generalized eigenvalues of block Toeplitz matrices. First, we detail three lemmas (Lemma 2-4) used in the proof of the theorem. The three lemmas are proved in [11] as well as Theorem 1.

**Lemma 2** Let  $\mathbf{A}_{n,m}$  be a Hermitian matrix with Toeplitz blocks generated by an absolutely summable sequence  $\{a_k^{u,v}\}_{k=-\infty,-1,0,1,\dots}$ . For all arbitrary eigenvalues  $\lambda(\mathbf{A}_{n,m})$  of  $\mathbf{A}_{n,m}$  we have

$$\min_{\omega, \lambda} \lambda(\mathbf{A}(\omega)) \leq \lambda(\mathbf{A}_{n,m}) \leq \max_{\omega, \lambda} \lambda(\mathbf{A}(\omega)).$$

Considering now a positive definite Hermitian block Toeplitz matrix, the following lemma is proved.

**Lemma 3** Let  $\mathbf{B}_{n,m}$  be a positive definite Hermitian matrix with Toeplitz blocks and absolutely summable sequences  $\{b_k^{u,v}\}_{k=-\infty,-1,0,1,\dots}$  and the associated asymptotically equivalent matrix  $\mathbf{C}_n(b)$  given by Lemma 1. If,  $\min_{\omega, \lambda} \lambda\{\mathbf{B}(\omega)\} = m_b > 0$ , then

$$\mathbf{B}_{n,m}^{-1} \sim \mathbf{C}_n^{-1}(b).$$

Then we also prove in [11] the following lemma used in the proof of Theorem 1.

**Lemma 4** With the assumptions of Lemma 3, if  $\mathbf{A}_{n,m}$  is a Hermitian matrix with Toeplitz blocks generated by an absolutely summable sequence  $\{a_k^{u,v}\}_{k=-\infty,-1,0,1,\dots}$  the associated matrices  $\mathbf{C}_n(a)$  and  $\mathbf{C}_n(b)$  given by Lemma 1 satisfy

$$\mathbf{B}_{n,m}^{-1} \mathbf{A}_{n,m} \sim \mathbf{C}_n^{-1}(b) \mathbf{C}_n(a).$$

Finally, we introduce the interval  $I_\omega = [\min_{\omega, \lambda} \lambda(\mathbf{B}^{-1}(\omega) \mathbf{A}(\omega)), \max_{\omega, \lambda} \lambda(\mathbf{B}^{-1}(\omega) \mathbf{A}(\omega))]$  and prove the following.

**Theorem 1** Let  $\mathbf{A}_{n,m}$  and  $\mathbf{B}_{n,m}$  be two Hermitian matrices with Toeplitz blocks, such that  $\mathbf{B}_{n,m}$  is positive definite, generated by absolutely summable sequences  $\{a_k^{u,v}\}_{k=-\infty,-1,0,1,\dots}$  and  $\{b_k^{u,v}\}_{k=-\infty,-1,0,1,\dots}$  respectively, with  $\min_{\omega, \lambda} \lambda\{\mathbf{B}(\omega)\} = m_b > 0$ . Then, for all continuous functions  $F$  on  $I_\omega$

$$\lim_{n \rightarrow \infty} \frac{1}{n} \sum_{k=1}^{mn} F(\lambda_k(\mathbf{A}_{n,m}, \mathbf{B}_{n,m})) = \frac{1}{2\pi} \int_{-\pi}^{\pi} \sum_{u=1}^m F(\lambda_u(\mathbf{A}(\omega), \mathbf{B}(\omega))) d\omega$$

As shown in [5, 12], and combined with the fact that, for all  $n$ , the eigenvalues of  $\mathbf{B}_{n,m}^{-1} \mathbf{A}_{n,m}$  lie in  $I_\omega$ , Theorem 1 leads to the following corollary [11]:

**Corollary 1** For any integer  $l$ , the smallest and the largest  $l$  generalized eigenvalues of  $(\mathbf{A}_{n,m}, \mathbf{B}_{n,m})$  are convergent in  $n$  and

$$\lim_{n \rightarrow \infty} \lambda_{mn-l+1}(\mathbf{A}_{n,m}, \mathbf{B}_{n,m}) = \min_{\omega} \lambda_m(\mathbf{A}(\omega), \mathbf{B}(\omega))$$

and

$$\lim_{n \rightarrow \infty} \lambda_l(\mathbf{A}_{n,m}, \mathbf{B}_{n,m}) = \max_{\omega} \lambda_l(\mathbf{A}(\omega), \mathbf{B}(\omega)).$$

#### 4. APPLICATION TO SPACE-TIME BEAMFORMING

Beamforming consists of spatially filtering signals, and allows one to form “nulls” in the direction of interfering sources while maintaining a given gain in a desired direction. Usually, signals are narrowband and spatial processing alone is sufficient. However, when signals are wideband, spatial beamforming performance degrades (see, e.g. [6, Chap. 6.13]). Some sort of frequency compensation is then required to keep good nulling performance. This can be achieved by either time-domain or frequency-domain implementations, whose performance depend on the signal and interference environments. In this work, we consider the time-domain implementation, using tapped delay lines (see, e.g., [9]). This implementation has been studied by many authors through numerical simulations [7, 9] for different weight optimization criteria. However, to the best of our knowledge, few analytical results exist in the case of the maximal SINR beamformer. Unlike the previous studies, our approach is asymptotic but can be applied for an arbitrary array with an arbitrary number of sensors.

As in [6], we assume that the output of each sensor has been quadrature demodulated and that the tap spacing is less than or equal to the Nyquist sampling rate  $\frac{1}{T} = B$  where  $B$  is the bandwidth of the signals. After recalling the expression of space-time covariance matrices, we show that the optimal space-time SINR can be interpreted as the maximum generalized eigenvalue of a block-Toeplitz matrix pair. Then, using Theorem 1 and Corollary 1, we study the asymptotic performance in terms of space-time beamforming SINR (w.r.t. the number of taps). Finally, we analyze the influence of the different implementation parameters and illustrate the results through numerical examples.

##### 4.1 Problem statement

Let consider an array composed of  $M$  sensors. We denote  $B$  the bandwidth of the signals around the center frequency  $f_0$ . Then, we consider an environment composed of a field of jammers, thermal noise and a target signal. The jammers and the thermal noise are modelled by non-zero bandwidth stationary processes and furthermore the thermal noise is spatially white, with power  $\sigma_n^2$ . The baseband jammers have power  $(\sigma_j^2)_{j=1..J}$  and power spectral density (PSD)  $(\mathcal{S}_j(f))_{j=1..J}$ . The jamming+noise  $M \times M$  spatial covariance matrix is equal to:

$$\bar{\mathbf{R}} = \int_{-\frac{B}{2}}^{\frac{B}{2}} \sum_{j=1}^J \mathcal{S}_j(f) \phi(\theta_j, f + f_0) \phi(\theta_j, f + f_0)^H df + \sigma_n^2 \mathbf{I}$$

with  $\phi(\theta_j, f + f_0) = [e^{jk\mathbf{r}_1^T \mathbf{i}(\theta_j)} \quad e^{jk\mathbf{r}_2^T \mathbf{i}(\theta_j)} \quad \dots \quad e^{jk\mathbf{r}_M^T \mathbf{i}(\theta_j)}]^T$  where  $(\mathbf{r}_m)_{m=1..M}$  denotes a vector pointing from an origin to the  $m^{\text{th}}$  array,  $\mathbf{i}(\theta_j)$  a unit length arrival vector for a jammer in the direction  $\theta_j$  and  $k = 2\pi \frac{c}{f + f_0}$  with  $c$  denoting the celerity of the wave. The target signal is also modelled by a non-zero bandwidth stationary process with PSD  $\mathcal{S}_S(f)$  and power  $\sigma_S^2$ . It is assumed to have a known DOA  $\theta_S$ . Its  $M \times M$  spatial covariance matrix may be written as

$$\bar{\mathbf{R}}_S = \int_{-\frac{B}{2}}^{\frac{B}{2}} \mathcal{S}_S(f) \phi(\theta_S, f + f_0) \phi(\theta_S, f + f_0)^H df.$$

##### 4.2 Expression of the space-time covariance matrices

Let  $N$  denote the number of taps used for space-time processing. The jamming+noise and target signal covariance matrices, respectively  $\bar{\mathbf{R}}_N$  and  $\bar{\mathbf{R}}_{S,N}$  are of dimension  $NM \times NM$ . Due to the stationarity of the processes, the space-time covariance matrices are block-Toeplitz structured and may be written as:

$$\begin{bmatrix} \mathbf{R}_0 & \mathbf{R}_1^H & \dots & \mathbf{R}_{N-1}^H \\ \mathbf{R}_1 & \ddots & \ddots & \mathbf{R}_{N-2}^H \\ \vdots & \ddots & \ddots & \vdots \\ \mathbf{R}_{N-1} & \mathbf{R}_{N-2} & \dots & \mathbf{R}_0 \end{bmatrix} \quad (3)$$

with

$$\mathbf{R}_n = \int_{-\frac{B}{2}}^{\frac{B}{2}} \left[ \sum_{j=1}^J \mathcal{S}_j(f) \phi(\theta_j, f + f_0) \phi(\theta_j, f + f_0)^H + \frac{\sigma_n^2}{B} \mathbf{I} \right] e^{-i2\pi n f T} df$$

and

$$\mathbf{R}_n = \int_{-\frac{B}{2}}^{\frac{B}{2}} \mathcal{S}_S(f) \phi(\theta_S, f + f_0) \phi(\theta_S, f + f_0)^H e^{-i2\pi n f T} df$$

with  $n = 0, \dots, N-1$ , for  $\bar{\mathbf{R}}_N$  and  $\bar{\mathbf{R}}_{S,N}$  respectively. Let note that the blocks are not necessarily Toeplitz, depending on the structure of the array. After introducing  $\omega = 2\pi f T$  and  $\omega_0 = 2\pi f_0 T$ , these two space-time covariance matrices are generated by the Fourier coefficients of the  $M \times M$  Hermitian matrix valued functions:

$$\mathbf{R}(\omega) = \begin{cases} \sum_{j=1}^J \mathcal{S}_j(\omega) \phi_j(\omega) \phi_j(\omega)^H + \sigma_n^2 \mathbf{I} & \text{for } |\omega| \leq \pi B T \\ 0 & \text{for } \pi B T \leq |\omega| \leq \pi \end{cases}$$

and

$$\mathbf{R}_S(\omega) = \begin{cases} \mathcal{S}_S(\omega) \phi_S(\omega) \phi_S(\omega)^H & \text{for } |\omega| \leq \pi B T \\ 0 & \text{for } \pi B T \leq |\omega| \leq \pi \end{cases}$$

with  $\mathcal{S}_j(\omega) \stackrel{\text{def}}{=} \frac{1}{T} \mathcal{S}_j(\frac{\omega}{2\pi T})$ ,  $\mathcal{S}_S(\omega) \stackrel{\text{def}}{=} \frac{1}{T} \mathcal{S}_S(\frac{\omega}{2\pi T})$ ,  $\phi_j(\omega) \stackrel{\text{def}}{=} \phi(\theta_j, \frac{\omega + \omega_0}{2\pi T})$  and  $\phi_S(\omega) \stackrel{\text{def}}{=} \phi(\theta_S, \frac{\omega + \omega_0}{2\pi T})$ .

##### 4.3 Asymptotic performance analysis

###### 4.3.1 Arbitrary jammers

Space-time beamforming consists in linearly filtering the data by a tap-stacked vector. We denote the filter  $\mathbf{w}_N$ , when  $N$  taps are used. In this work, we consider the maximal SINR filter optimization criterion. The optimal space-time processing (in the sense of SINR maximization) maximizes the generalized Rayleigh quotient:

$$\text{SINR}(N) \stackrel{\text{def}}{=} \max_{\mathbf{w}_N} \frac{\mathbf{w}_N^H \bar{\mathbf{R}}_{S,N} \mathbf{w}_N}{\mathbf{w}_N^H \bar{\mathbf{R}}_N \mathbf{w}_N} \quad (4)$$

where  $\bar{\mathbf{R}}_{S,N}$  and  $\bar{\mathbf{R}}_N$  are the space-time covariance matrices for the target and jamming+noise signals, respectively, and given by (3). As noted in Section 2.2,  $\bar{\mathbf{R}}_{S,N}$  and  $\bar{\mathbf{R}}_N$  are, respectively, Hermitian positive semidefinite and Hermitian positive definite matrices. Therefore, the solution of this optimization problem is given by the principal generalized eigenvector of these two matrices, or equivalently  $\mathbf{w}_N \propto \mathcal{P}(\bar{\mathbf{R}}_N^{-1} \bar{\mathbf{R}}_{S,N})$  where  $\mathcal{P}(\cdot)$  stands for the eigenvector associated with the largest eigenvalue of a matrix. Then, the optimal space-time SINR is given by the largest generalized eigenvalue of  $\bar{\mathbf{R}}_{S,N}$  and  $\bar{\mathbf{R}}_N$ . Noting that the space-time setting with  $N$  taps is a special case of a processor with  $N+1$  taps, where the  $N+1$ st tap weight is set to zero in each channel, we obtain by the inclusion principle in (4) that the SINR is an increasing function of the number of taps.

We consider in the following the limit of the SINR w.r.t.  $N$  for arbitrary given jammer and target DOAs. In the case where  $T = \frac{1}{B}$ , the assumptions of Theorem 1 and Corollary 1 apply for the sequence of the space-time covariance matrices  $(\bar{\mathbf{R}}_{S,N}, \bar{\mathbf{R}}_N)$  w.r.t. the number of taps:

$$\lim_{N \rightarrow \infty} \text{SINR}(N) = \max_{\lambda, f \in [-\frac{B}{2}, \frac{B}{2}]} \{\lambda(\mathbf{R}^{-1}(f)\mathbf{R}_S(f))\}$$

where

$$\mathbf{R}(f) = \sum_{j=1}^J \mathcal{S}_j(f) \phi(\theta_j, f + f_0) \phi(\theta_j, f + f_0)^H + \frac{\sigma_n^2}{B} \mathbf{I} \quad (5)$$

and

$$\mathbf{R}_S(f) = \mathcal{S}_S(f) \phi(\theta_S, f + f_0) \phi(\theta_S, f + f_0)^H.$$

Then, since  $\mathbf{R}^{-1}(f)\mathbf{R}_S(f)$  has rank one, it has a single non-zero eigenvalue

$$\mathcal{S}_S(f) \phi(\theta_S, f + f_0)^H \mathbf{R}^{-1}(f) \phi(\theta_S, f + f_0)$$

and we obtain the following result:

**Result 1** For optimal space-time beamforming sampled at the Nyquist rate, the SINR tends to the maximal zero-bandwidth optimal spatial SINR associated with a frequency in the band  $I_f = [-\frac{B}{2}, \frac{B}{2}]$  when the number of taps increases to  $\infty$ .

$$\lim_{N \rightarrow \infty} \text{SINR}(N) = \max_{f \in I_f} \{\mathcal{S}_S(f) \phi(\theta_S, f + f_0)^H \mathbf{R}^{-1}(f) \phi(\theta_S, f + f_0)\} \quad (6)$$

with  $\mathbf{R}(f)$  given by (5).

Let note that the asymptotic (in the number of taps) space-time SINR (6) can be interpreted as the maximal zero-bandwidth optimal (in the sense of SINR maximization) spatial SINR w.r.t. frequency in the band  $I_f$ . Consequently, it has the same behavior as an infinitely narrow bandpass filter (at the frequency solution of the maximization (6)) followed by a zero-bandwidth adaptive beamformer. Therefore, it can outperform the zero-bandwidth optimal spatial SINR which corresponds to the frequency  $f = 0$ .

In the case  $T < \frac{1}{B}$ , the spectral matrices  $\mathbf{R}_S(\omega)$  and  $\mathbf{R}(\omega)$  are bandlimited to  $[-\pi BT, \pi BT]$ , so  $\min_{\lambda, \omega} \lambda(\mathbf{R}(\omega)) = 0$  and the assumptions and the statements of Theorem 1 and Corollary 1 are no longer valid. Extension of Corollary 1 in the subband  $[-\pi BT, \pi BT]$  is thus challenging. However, extensive numerical experiments show that Result 1 extends to that case (see Subsection 4.4.1).

In the following, we suppose that the signal is white so that  $\mathcal{S}_S(f) = \frac{\sigma_s^2}{B}$ . We now analyze the particular situation of jammers whose spectra cancel at least at a common frequency.

#### 4.3.2 Jammers whose spectra cancel at least at a common frequency

In this particular case, we obtain the following result:

**Result 2** In the presence of several jammers whose spectra cancel at least at a common frequency and a white signal, we have

$$\lim_{N \rightarrow \infty} \text{SINR}(N) = \frac{\sigma_s^2}{\sigma_n^2} M.$$

This result means that in the presence of jammers with at least one common zero in their spectrum, space-time processing allows one to reach asymptotically the SINR corresponding to a jammer-free context. Let note that though the asymptotic notion is purely theoretical, we will see in Subsection 4.4.2 that in most practical cases, a small number of taps is sufficient to reach near optimal performance.

#### 4.4 Illustrative examples

We now illustrate Results 1 and 2 through numerical experiments. We consider throughout this section a uniform linear array (ULA) with only one jammer where

$$\phi(\theta, f) = \begin{bmatrix} 1 & e^{j\pi \frac{f}{f_u} u} & \dots & e^{j(M-1)\pi \frac{f}{f_u} u} \end{bmatrix} \quad (7)$$

with  $u = \sin(\theta)$  ( $u_S = \sin(\theta_S)$  and  $u_J = \sin(\theta_J)$  for the target signal and the jammer respectively) and where  $f_u$  depends on the choice of the inter-element spacing. The parameters of the simulation are  $\frac{B}{f_0} = 0.3$ ,  $M = 16$ ,  $u_J = 0.3$ ,  $\sigma_J^2 = 30$  dB and  $\sigma_S^2 = 0$  dB.

##### 4.4.1 White jammer case

In this Section, we suppose that the jammer is white in the band  $[-\frac{B}{2}, \frac{B}{2}]$ .

**Influence of the time sampling frequency** Now, we examine the influence of the time sampling rate on the optimal space-time SINR. In Fig. 1, we plot the optimal space-time SINR for two values of the temporal sampling period, i.e.  $T = \frac{1}{B}$  and  $T = \frac{1}{2B}$  and different values of the number of taps. First, we observe that in both cases, the SINR seems to converge to the asymptotic SINR given by Result 1, although this result has been proved only for  $T = \frac{1}{B}$ . However, we note that the convergence is much faster for  $T = \frac{1}{2B}$  than for  $T = \frac{1}{B}$ . Consequently, oversampling w.r.t. the Nyquist sampling rate allows one to improve the performance for a given number of taps. We note that extensive experiment confirms these observations. Let us note that the influence of the time sampling rate has been analyzed in [8] for a bandpass tapped delay line implementation of the MMSE algorithm in the case of a two-sensor array. In this paper, we have also noticed the improvement of performance in terms of SINR due to the use of oversampling, for an array in which each element has only two weights. The physical interpretation is that oversampling increases the correlation between interference components which makes their nulling easier.

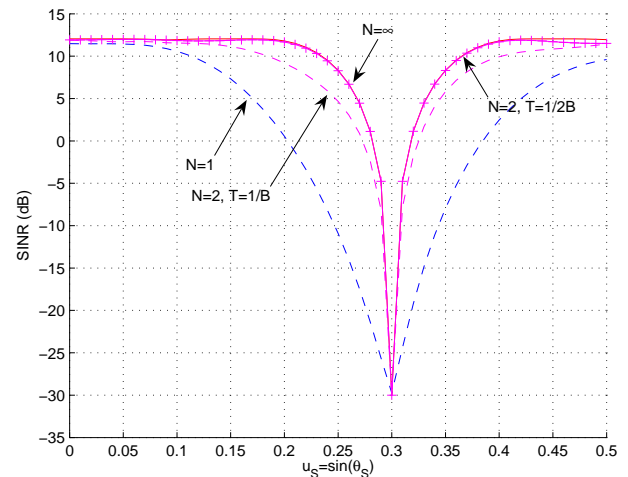


Fig. 1: Optimal space-time SINR with  $T = \frac{1}{B}$  (- -) and  $T = \frac{1}{2B}$  (-+ -) for different values of the number of taps, as a function of the target's DOA.

**Influence of the spatial sampling frequency** Now, we examine the influence of the inter-sensor spacing equal to  $\frac{c}{2f_u}$  (see (7)). In order to respect the Shannon sampling condition, the parameter  $f_u$  must be at least equal to the maximum frequency of the signal, i.e.  $f_u = f_0 + \frac{B}{2}$ . This corresponds to an inter-element spacing less than or equal to  $\frac{c}{2(f_0 + \frac{B}{2})}$ . However, in some practical cases, the array may not be required to steer the entire visible region, i.e.  $90^\circ \leq \theta \leq 90^\circ$ . Therefore, a greater inter-element spacing can be allowed, at the price of a reduced detection domain. Indeed, not respecting the Shannon sampling condition leads to the occurrence of grating lobes at some frequencies, but they can be kept out of the visible region if the array steering domain is sufficiently limited [6, Chap. 2.5]. Here, we analyze the influence of  $f_u$  on the asymptotic optimal space-time SINR. More precisely, we compare the choice of  $f_u = f_0$  with the sampling frequency  $f_u = f_0 + \frac{B}{2}$  for which the Shannon sampling condition is respected. To compare both considered cases, we plot in Fig. 2 the ratio between the optimal zero-bandwidth spatial SINR  $\text{SINR}_{ZB} = \sigma_S^2 \phi(\theta_S, f_0)^H \mathbf{R}^{-1} \phi(\theta_S, f_0)$  with  $\mathbf{R} = \sigma_J^2 \phi(\theta_J, f_0) \phi(\theta_J, f_0)^H + \sigma_n^2 \mathbf{I}$  and the asymptotic optimal space-time SINR for  $f_u = f_0$  and  $f_u = f_0 + \frac{B}{2}$ . First, we observe that the two plots are upper-bounded by 1. The asymptotic optimal space-time filter outperforms the optimal spatial filter for arbitrary given

jammer and target DOAs. Then, we note that for a target in a large vicinity of the jammer, the asymptotic optimal space-time SINR with  $f_0 = f_u$  is greater than with  $f_u = f_0 + \frac{B}{2}$  while the behavior of this asymptotic space-time SINR does not degrade significantly for a target "far" from the jammer. Consequently, the choice  $f_u = f_0$  improves the performance w.r.t. the Shannon sampling frequency.

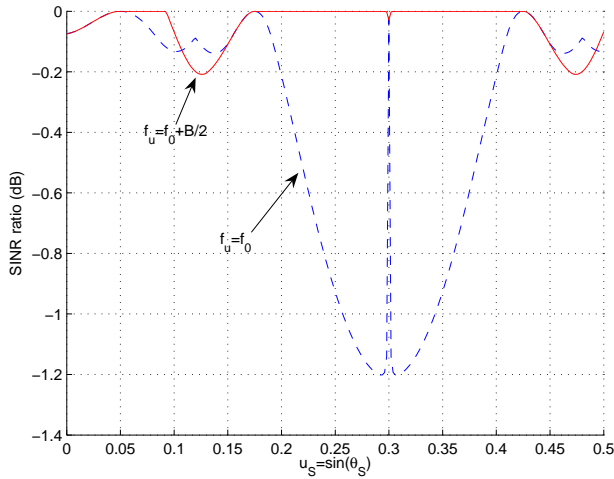


Fig.2: Ratio between the optimal spatial SINR and the asymptotic optimal space-time SINR for two inter-sensor spacings, as a function of the target's DOA.

#### 4.4.2 Bandlimited jammer case

Let suppose that the jammer has constant PSD in the band  $[-\frac{b}{2}; \frac{b}{2}]$  with  $b < B$ . Note that in this case,  $\mathbf{R}(\omega)$  remains nonsingular and thus Result 2 applies. Here, we illustrate the speed of convergence of the optimal space-time SINR for a given number of taps to the asymptotic upper-bound given by Result 2. Thus, we plot in Figs.3 and 4 the optimal space-time SINRs for  $b = \frac{3}{4}B$  and  $b = \frac{B}{2}$  respectively (dashed plots) at given numbers of taps and compare them to the asymptotic optimal space-time SINR (solid plot). Let note that the case  $N = 1$  corresponds to spatial processing and that the SINR degrades when  $b$  increases. In both figures, we check that the optimal SINR (asymptotically w.r.t. the number of taps) is equal to  $\frac{\sigma_s^2}{\sigma_j^2}M$  and that the optimal space-time SINRs converge with the number of taps to the asymptotic optimal space-time SINR. Then, we note that the convergence speed increases when the jammer bandwidth decreases.

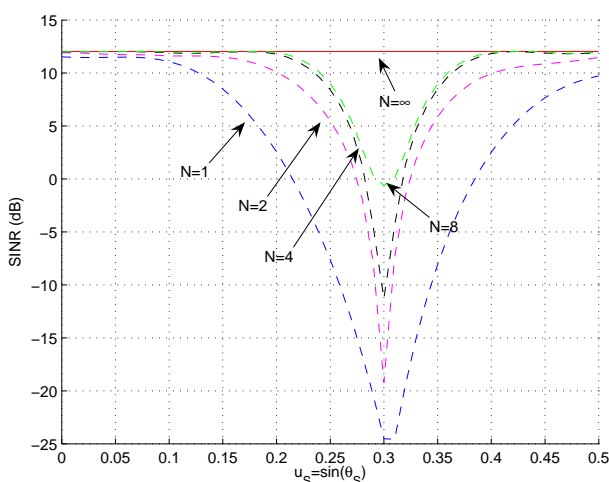


Fig.3: Optimal space-time SINR for different values of the number of taps, as a function of the target's DOA for  $b = \frac{3B}{4}$ .

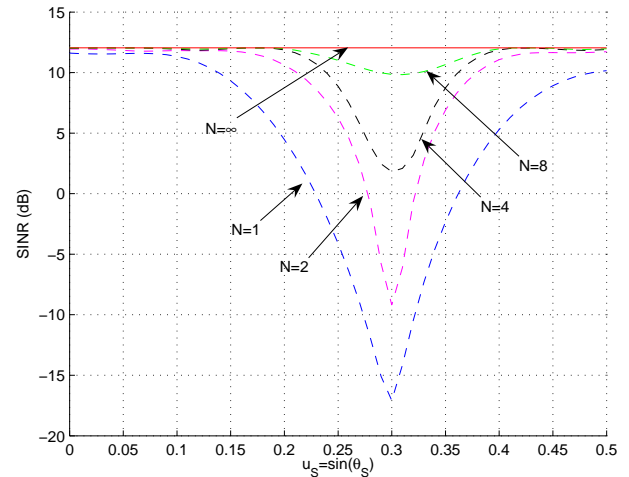


Fig.4: Optimal space-time SINR for different values of the number of taps, as a function of the target's DOA for  $b = \frac{B}{2}$ .

For instance, we observe in Fig.4 (where  $b = \frac{B}{2}$ ) that the optimal space-time SINR with  $N = 4$  taps outperforms the optimal space-time SINR with  $N = 8$  taps of Fig.3 (where  $b = \frac{3B}{4}$ ).

#### REFERENCES

- [1] P. Tilli, "Asymptotic spectral distributions of Toeplitz-related matrices," in *Fast Reliable Algorithms for Matrices with Structure*, T. Kailath and A. H. Sayed, Eds. Philadelphia, PA: SIAM, pp. 153-187, 1999.
- [2] P. Tilli, "Singular values and eigenvalues of non-Hermitian block Toeplitz matrices," *Linear Algebra Its Appl.*, vol. 271, pp. 59-89, 1998.
- [3] M. Miranda and P. Tilli, "Asymptotic spectra of Hermitian block Toeplitz matrices and preconditioning results," *SIAM J. Matrix Anal. Applic.*, vol. 21, pp. 867-881, 2000.
- [4] U. Grenander and G. Szegö, *Toeplitz Forms and Their Applications*. New York: Chelsea, 1984.
- [5] R.M. Gray, "On the asymptotic eigenvalue distribution of Toeplitz matrices," *IEEE Trans. Inform. Theory*, vol. 18, pp. 725-730, Nov. 1972.
- [6] H.L. Van Trees, *Optimum array processing, part IV of Detection, Estimation and Modulation Theory*, Wiley Interscience, New York, 2002.
- [7] W.E. Rodgers, R.T. Compton, "Adaptive array bandwidth with tapped delay-line processing," *IEEE Trans. Aerospace Electron. Syst.*, vol. 15, pp. 21-27, Jan. 1979.
- [8] R.T. Compton, "The bandwidth performance of a two-element adaptive array with tapped delay-line processing," *IEEE Trans. Antennas Propagat.*, vol. 36, pp. 5-14, Jan. 1988.
- [9] J.T. Mayhan, A.J. Simmon, W.C. Cummings, "Wideband adaptive antenna nulling using tapped delay-lines," *IEEE Trans. Antennas Propagat.*, vol. 29, pp. 923-936, Nov. 1981.
- [10] H. Gazzah, P.A. Regalia, J.P. Delmas, "Asymptotic eigenvalue distribution of block Toeplitz matrices and applications to blind SIMO channel identification," *IEEE Trans. Inform. Theory*, vol. 47, pp. 1243-1241, Jan. 2001.
- [11] M. Oudin, J-P. Delmas, "Asymptotic generalized eigenvalue distribution of block Toeplitz matrices and application to space-time beamforming", submitted to *IEEE Trans. Signal Process.*
- [12] R.M. Gray, "Toeplitz and circulant matrices : a review," *Foundations and Trends in Communications and Information Theory*, vol. 2, pp. 155-239, 2006.